

1 Novel crAssphage isolates exhibit conserved gene order and purifying
2 selection of the host specificity protein

3 New crAssphage isolates infecting *Bacteroides cellulosilyticus* WH2

4 Bhavya Papudeshi¹, Alejandro A. Vega², Cole Souza², Sarah K. Giles¹, Vijini
5 Mallawaarachchi¹, Michael J. Roach¹, Michelle An², Nicole Jacobson², Katelyn McNair
6 ², Maria Fernanda Mora², Karina Pastrana², Christopher Leigh³, Clarice Cram¹, Will S.
7 Plewa¹, Susanna R. Grigson¹, George Bouras⁶, Przemysław Decewicz^{4,1}, Antoni
8 Luque^{7,8}, Lindsay Droit⁵, Scott A. Handley⁵, Anca M. Segall², Elizabeth A. Dinsdale¹,
9 Robert A. Edwards¹

10 ¹Flinders Accelerator for Microbiome Exploration, College of Science and Engineering,
11 Flinders University, Bedford Park, Adelaide, SA, 5042, Australia

12 ²Department of Biology, San Diego State University, 5500 Campanile Drive, San Diego,
13 CA, 92182, USA

14 ³Adelaide Microscopy, University of Adelaide, Adelaide, SA, 5005, Australia

15 ⁴Department of Environmental Microbiology and Biotechnology, Institute of
16 Microbiology, Faculty of Biology, University of Warsaw, Miecznikowa 1, Warsaw, 02-
17 096, Poland

18 ⁵Department of Pathology & Immunology, Washington University School of Medicine,
19 St. Louis, MO, 63110, USA

20 ⁶Adelaide Medical School, Faculty of Health and Medical Sciences, The University of
21 Adelaide, Adelaide, SA, 5005, Australia.

22 ⁷Department of Mathematics and Statistics, San Diego State University, 5500
23 Campanile Drive, San Diego, CA, 992182, USA

24 ⁸Computational Science Research Center, San Diego State University, 5500 Campanile
25 Drive, San Diego, CA, 992182, USA

26 *Corresponding author: Bhavya Papudeshi, nala0006@flinders.edu.au

27

28

29

30

31

32

33

34

35

36 Abstract

37 Bacteroidota are the most common bacteria in the human gut and are responsible for
38 degrading complex polysaccharides that would otherwise remain undigested. The
39 abundance of Bacteroides in the gut is shaped by phages such as crAssphages that
40 infect and kill them. While close to 600 genomes have been identified computationally,
41 only four have been successfully cultured. Here, we identify and characterize three
42 novel crAssphage species isolated from wastewater and infecting the bacterial host
43 *Bacteroides cellulosilyticus* WH2. We named the novel species, *Kehishuvirus winsdale*
44 (Bc01), *Kolpuevirus frerule* (Bc03), and *Rudgehvirus redwords* (Bc11) which span two
45 different families and three genera. These phages may not have co-evolved with their
46 respective bacterial hosts. The phages had a conserved gene arrangement with known
47 crAssphages, but gene similarity within phages belonging to the same taxa was highly
48 variable. Across the three species, only two structural genes encoding a hypothetical
49 protein and a tail spike protein were similar. Evolutionary analysis revealed the tail spike
50 protein is undergoing purifying selection and was predicted to bind to a TonB-dependent
51 transporter on the host cell surface, suggesting a role for host specificity. This study
52 expands the known crAssphage isolates and reveals insights into the crAssphage
53 infection mechanism. The availability of pure cultures of multiple crAssphage infecting
54 the same host provides an opportunity to perform controlled experiments on one of the
55 most dominant members of the human enteric virome.

56

57

58 Introduction

59 There is an intricate relationship between gut microbiomes and human health. A healthy
60 gut microbiome contains a high diversity of microbes that help with digestion, regulate
61 the immune system, and alter brain function (1–3). Application of the metagenomics
62 technique, a culture-independent technique that captures the diversity of the microbial
63 community in a sample (4,5) has transformed our understanding of the prevalence of
64 bacteria and the corresponding bacteriophages in the environment (6–9). From
65 metagenomic datasets, we have observed a correlation between bacterial and
66 bacteriophage populations which suggests bacteriophages play a role in controlling the
67 ratios of different bacteria (10,11). For instance, within an environment with high or low
68 bacterial densities, phages favor integration into the bacterial host, while at intermediary
69 densities the phages favor host lysis (12). The human gut microbiome has high bacterial
70 densities, including a high abundance of Bacteroidota (formerly Bacteroidetes) (13–15),
71 which are shaped by the phages that infect and kill them such as crAssphages. The
72 dsDNA crAssphages have a podovirus-like morphology, genomes ranging between 100
73 and 200 kb, and conserved gene order (16–18). These bacteriophages are ubiquitous,
74 can stably colonize an individual, and do not appear to be associated with health or
75 disease states (17,19). This phage was first discovered computationally by cross-
76 assembling DNA sequence reads from human gut microbiome samples (20), and to
77 date, there have been close to 600 crAssphage genomes identified computationally, but
78 only four cultured phages (16,21).

79 The isolation of crAssphages *in vitro* remains a challenge with only four successful pure
80 isolates after eight years of experimental research. In 2018, *Kehishuvirus primarius*

81 (crAss001) was isolated from *Bacteroides intestinalis* (22). A brace of phages,
82 *Wulhauvirus bangladeshii* DAC15 and DAC17, were isolated from wastewater effluent
83 infecting *Bacteroides thetaiotaomicron* (23). Finally, *Jahgtovirus secundus* (crAss002)
84 was isolated on *Bacteroides xylanisolvans* (24). All the pure isolates exhibited host
85 specialist morphotypes that can be maintained in the continuous host culture, but none
86 possess lysogeny-related genes to suggest a lysogeny lifestyle (22,25). Alternative
87 mechanism proposed is that these phages host populations cycle between sensitive
88 and resistant states through phase variation of capsular polysaccharides or through
89 exhibiting pseudolysogeny or a carrier state phenotype (25). Transmission electron
90 microscopy (TEM) of these phages has confirmed podovirus-like morphology
91 (22,24,26).

92 Analysis of all known crAssphage that includes the pure cultures and the
93 computationally identified crAssphage led to grouping of these phages to distinct group.
94 Recently, International Committee of Taxonomy of Viruses (ICTV) published a formal
95 report on classification of Crassvirales order into four families, ten subfamilies, 42 new
96 genera, and 72 new species (18,27). This classification was based on phylogenetic
97 analysis of conserved structural genes, such as major capsid protein (MCP), terminase
98 large subunit (*terL*), and portal protein (portal). Despite this progress and expansion of
99 the Crassvirales order, functional annotation of viral genome remains challenging, with
100 lots of genes annotated as hypothetical proteins with no known biological function.
101 However, subsequent analysis with the Crassvirales has improved our understanding of
102 phage diversity, and revealed their unique biological characteristics (28,29). For
103 instance, these genomes contain three discernible regions encoding for 1) structural

104 proteins involved in producing the capsid and tail genes, 2) transcription proteins and 3)
105 replication proteins that are involved in the successful replication of the phage that is
106 activated in the different stages of phage infection (16). They also revealed unique
107 characteristics of the lineage including switching DNA polymerases, alternative coding
108 strategies (30–33), and the variable density of introns across taxa (16,33). Further,
109 cryogenic-electron microscopy of *K. primarius* (crAss001) added the structural basis of
110 the genes and description of the mechanisms of assembly and infection (26). An
111 evolutionary study of crAssphages showed that capsid protein is the most conserved
112 gene, followed by two other uncharacterized proteins within the structural module (18).
113 The remaining modules are highly variable with little homology to other known proteins.
114 Here we present the isolation and characterization of three novel crAssphage isolates
115 from wastewater. We present three new species within *Steigviridae* and *Intestiviridae*
116 families and how they infect the same host, *Bacteroides cellulosilyticus* WH2. We
117 computationally predict the genes playing a role in host specificity, providing insights
118 into the evolution of these dominant phages, and how their interactions shape the gut
119 microbiome.

120 **Results**

121 Isolation and assembly of phage genomes *B. cellulosilyticus* WH2
122 We isolated and sequenced 16 *B. cellulosilyticus* WH2 phage isolates, with phage
123 (Bc01 to Bc12) genomes sequenced on the Oxford Nanopore platform assembled using
124 Flye and Unicycler, while genomes (Bc01 to Bc08, Bc13 to Bc16) sequenced on the

125 Illumina platform were assembled using MEGAHIT assembly. We used multiple
126 assemblers as bioinformatics assembly tools have some level of algorithmic nuances as
127 well as sensitivities to different features (Table S1). For each genome, our selection
128 criterion (viral, highest read coverage, unitig approximately 100kb) identified as
129 complete phage genome for 14 of the 16 phage samples across both sequencing
130 platforms (Table S1). Two genomes (Bc04, Bc12) did not assemble due to their
131 coverage profile (Figure S1), were also identified to be replicates of other assembled
132 genomes and therefore left out of this analysis. Finally, the 14 phage genomes from the
133 Nanopore based assembly were polished with Illumina reads correcting for substitution,
134 insertion, and deletion errors (Table S1). These assembled unitigs were then processed
135 to calculate the average nucleotide identity (ANI) (part of CrassUS workflow), and
136 genomes with more than 95% ANI were grouped as likely phage replicates (Table S1).
137 This reduced our phage genomes to three clusters of phages from which we selected
138 the highest confidence genomes: Bc01, Bc03, and Bc11.

139 Taxonomic assignment of the three novel isolates

140 To identify the taxa of the three representative isolates, BLASTN searches were
141 performed against the non-redundant (nr/nt) NCBI database confirming that all three
142 representative isolates (Bc01, Bc03 and Bc11) were crAssphage (34). The phylogenetic
143 tree built from conserved proteins including the major capsid protein (MCP), portal,
144 terminase large subunits (*terL*) genes from all 14 assembled phage genomes
145 demonstrated that Bc01 and Bc03 belong to the *Steigviridae* family, and Bc11 to the
146 *Intestiviridae* family (Figure 1, Figure S2). The taxonomic classification follows the ICTV
147 report with suggestions on defining a taxonomy for phage genomes belonging to the

148 Crassvirales order. Taxonomic classification of the three genomes was also confirmed
149 with ANI and shared protein information, identifying Bc01 to belong to *Kehishuvirus*,
150 Bc03 to *Kolpuevirus*, and Bc11 to a novel genus group that we propose to call
151 *Rudgehvirus*.

152 All three isolates are novel species exhibited less than 95% identity to any known
153 crAssphage genome. Bc01 is most similar to the reference genome *Kehishuvirus*
154 *primarius* (crAss001, MH675552) with 95.5% identity across 79.1% genome coverage.
155 Bc03 aligns with *Kolpuevirus hominis* (crAssphage cr126_1, MT774391) with 82.8%
156 identified across 53.73% query coverage. Bc11 aligns with the reference genome
157 *Jahgtovirus intestinalis* (OGOL01000109) with 74.7% identity across only 9.9% query
158 coverage. We named these novel species *Kehishuvirus winsdale* (Bc01), *Kolpuevirus*
159 *frurule* (Bc03), and *Rudgehvirus redwords* (Bc11) (Table 1).

160 Table 1: Genome characteristics of the three novel crAssphage representative isolates
161 Figure 1: Phylogenetic tree of the portal protein showing that isolate *K. winsdale* (Bc01)
162 and *K. frurule* (Bc03) belong to the family *Steigviridae* (cyan), and *R. redwords* (Bc11) to
163 *Intestiviridae* (red). The outgroup is set to *Cellulophaga phage phi13:2*.

164 Genome characteristics of the novel species

165 *Kehishuvirus winsdale* (Bc01) is 100,841 bp, with 104 proteins and 24 tRNAs identified
166 within the genome (Table 1). The cumulative GC% of this genome is 35.09% (Table 1)
167 which is lower than the bacterial host GC% of 42.8%. This genome is 95% similar to the
168 isolate *K. primarius* (crAss001). In a few crAssphage genomes, a direct terminal repeat
169 has been proposed to be involved in genome packaging (including *K. primarius*) but no

170 direct terminal repeat was identified in *K. winsdale*. There was also no evidence of stop
171 codon reassignment in this genome as observed in closely related reference *K.*
172 *primarius* (Table S2). While 24 tRNA genes were identified within a contiguous segment
173 from 88,172 to 93,727 bp on the genome, no tRNA suppressors were found that would
174 be used to stop codon reassignment (Table S2). Functional gene annotations were
175 performed by aligning the 104 predicted genes across all the known Caudovirales
176 genomes and generating functional assignments for 48 genes (Table S3). From the
177 functional assignments, we were able to divide the genome into three regions
178 (structural, transcription, and replication) as observed across all the other crAssphage
179 genomes (Figure 2). There was no lysogeny module or integrase-related genes
180 detected within the phage genome and there was no evidence of temperate replication
181 in the plaque morphology.

182 *Kolpuevirus frerule* (Bc03) belonged to the same family, *Steigviridae* as *K. winsdale*
183 (Bc01). This genome was shorter in length (99,523 bp) but with a similar GC content of
184 33% (Table 1). This genome is 82% similar to a reference genome to this isolate
185 *Kolpuevirus hominis* (CrAssphage cr126_1). Neither direct terminal repeat genome
186 packaging, stop-codon reassignment, nor integration and lysogeny were observed
187 (Table S2). Functional characterization of this genome predicted 108 genes, of which 45
188 were assigned a function (Table S4). In this genome, only four tRNA genes were
189 predicted, two coding for arginine (TCT anticodon), and the other two encoding
190 asparagine (GTT anticodon), and tyrosine (GTA anticodon).

191 Finally, *Rudgehvirus redwords* (Bc11) is 90,575 bp in length with 29.15% GC, and there
192 were 84 genes encoded within this genome (Table 1). Taxonomic assignment of this

193 genome placed this isolate within the *Intestiviridae* family, but in a novel genus.
194 Currently, this genus includes only this isolate (Figure 1), with the neighboring clade
195 including *Jahgtovirus* crAssphages. We named the new genus *Rudgehvirus* following
196 the ICTV Caudovirales order naming suggestions. The reference genome that is most
197 closely related to this genome is *Jahgtovirus intestinalis* (uncultured phage cr54_1) with
198 75%. In addition, pure culture isolate crass002 (*J. secundus*) also belongs to the closely
199 related clade. There were 84 predicted genes with standard stop codons, as there was
200 no evidence of codon reassignment (Table S2), and 36 of these genes were assigned a
201 function (Table S4). Similar to one-third of crAssphage genomes currently known, there
202 were no tRNA genes (Table S2) identified in this genome.

203 We compared the gene arrangement across the three novel species by comparing gene
204 similarity with clinker (only greater than 30%) and demonstrated that *Steigviridae* (Bc01,
205 Bc03) isolates shared more gene similarity compared to *Intestiviridae* (Bc11) in
206 congruence with taxa classification (Figure 2). Across the three isolates, there were only
207 three shared genes: two encoding structural proteins, and one hypothetical gene within
208 replication machinery. *Steigviridae* isolates shared 68 genes: 24 belonging to the
209 structural region; none within the transcription machinery; and the remaining 44 genes
210 within the replication machinery. Finally, *Kehishuvirus* (Bc01) and *Rudgehvirus* (Bc11),
211 and *Kolpuevirus* (Bc03) and *Rudgehvirus* (Bc11) shared two structural genes along with
212 one hypothetical gene within the replication machinery.

213 Figure 2: A) Transmission electron microscopy images negatively stained with uranyl
214 acetate of the three isolates, *K. winsdale* (Bc01), *K. frerule* (Bc03), and *R. redwords*
215 (Bc11). B) Gene arrangement and functional annotation of the three genomes color-

216 coded based on their functional modules and hypothetical genes represented in white.
217 The direction of the arrows represents the direction of the gene read from the genome,
218 and the arrows themselves represent individual genes. The links connecting the genes
219 indicate sequence identity, ranging from 30% (grey) to 100% (black).

220 Podovirus-like morphology

221 Transmission electron microscopy (TEM) of the three species revealed all have a
222 podovirus-like morphology (Figure 2). *K. winsdale* (Bc01) displayed polyhedral capsids
223 with a diameter of 94 ± 3 nm, tails with collar structures that were 34 ± 3 nm with
224 several tail fibers with variable lengths. *K. frerule* (Bc03) included capsids of diameter
225 97 ± 3 nm, a tail with collar structures of 33 ± 3 nm, and several tail appendages of
226 variable length. Finally, *R. redwords* (Bc11) was slightly smaller in size with capsids of
227 size 90 ± 4 nm, tails with collar structures measuring 25 ± 4 nm, with tail appendages
228 that were of variable length but different tail structure than the other two crAssphage
229 genomes.

230 Synteny across crAssphages

231 Comparing the three new species from this study with the four reference crAssphage
232 isolates available showed gene similarity expected from the taxonomic assignment.
233 Within the *Steigviridae* genomes including two new species and three reference
234 genomes, *K. winsdale* (Bc01) was most similar to *K. primarius* (crAss001) sharing 76 of
235 106 genes, and two isolates belonging to the *Wulhauvirus* genus (DAC15 and DAC17)
236 shared 115 of the 121 genes with the highest similarity. Meanwhile, *K. frerule* (Bc03)
237 was equidistant from the species of *Kehishuvirus* (68 genes shared) and *Wulhauvirus*

238 genus (71 genes) (Figure 3A). The third isolate *R. redwards* (Bc11) was compared to
239 the *J. secundus* (crAss002) as these two isolates belonged to an *Intestiviridae* family,
240 and they shared 37 genes including 11 structural genes, three transcription genes, and
241 23 replication-related genes (Figure 3B). However, they are both overall dissimilar to
242 genomes from *Steigviridae* (Figure 3A). A notable characteristic was that tail-related
243 genes were only shared by those isolates infecting the same host. *K. winsdale* (Bc01),
244 *K. frurule* (Bc03) and *R. redwords* (Bc11) shared unique tail-related genes although they
245 belonged to different genera (Figure 2).

246 Figure 3. Gene synteny across seven pure culture isolates across two crAssphage
247 families A) *Steigviridae* family comprising five isolates spanning across three genera B)
248 *Intestiviridae* family comprising two isolates from two genera. The arrows represent
249 genes, with their direction indicating the gene direction, and their color indicating cluster
250 group with the grey-colored arrows representing unique genes that didn't form any
251 clusters. The functional color coding for A and B are different. Finally, the links
252 connecting the genes are color-coded based on sequence similarity, ranging from grey
253 (30%) to black (100%). New isolates included in this study are represented with * next
254 to their name, and the tail proteins that were shared between the three isolates from this
255 study are highlighted with a red box.

256 Structural proteins playing a role in host specificity

257 To test if the common genes across the three new species in this study play a role in
258 host specificity, we performed evolutionary analyses comparing 1,887 genes across the
259 14 crAssphage isolates from this study along with four reference genomes. Overall,

260 1,766 of them were categorized into 383 orthologous groups (Table S6), and the
261 remaining 121 genes were singletons. We identified 64 orthogroups (193 genes) that
262 were specific to *Kehishuvirus*, 55 orthogroups (564 genes) specific to *Kolpuevirus*, 89
263 orthogroups (187 genes) specific to *Wulhauvirus*, 73 orthogroups (148 genes) specific
264 to *Rudgehvirus*, and 5 orthogroups (10 genes) specific to *Jahgtovirus* genera. Testing
265 for host-specificity within each of these groups only identified two orthogroups—
266 OG000000 (including Bc01 protein gp23) and OG000008 (including Bc01 protein
267 gp22)—encoding a hypothetical gene and tail spike protein within the structural block,
268 which only included genes from crAssphage isolates that infect *B. cellulosilyticus* WH2
269 (Table 2). These two orthogroups also represent the two tail proteins that were common
270 across the three new isolates in this study (Figure 3).

271 Calculating the number of synonymous (d_S) and non-synonymous (d_N) mutations
272 occurring within the orthogroups reflected $d_N/d_S < 1$, suggesting purifying selection.
273 Averaging all the sequence pairs, we used the codon-based z-test to identify genes
274 under selection and found that OG000000 followed the null hypothesis (z-score=0.56, p-
275 value=0.29) suggesting that the gene is under neutral evolution, while OG000008
276 rejected the null hypothesis (z-score=0.56, p-value<0.001), suggesting that the gene is
277 under purifying selection.

278 Table 2: Inferred selection of the three orthogroups with genes from all crAssphage
279 isolates infecting the host *B. cellulosilyticus*. Orthogroups under purifying selection are
280 represented with an asterisk (*)

281 Prediction of the phage receptor binding domain

282 The predicted structure of all 103 proteins from *K. winsdale* (Bc01) were generated
283 using Colabfold (35) (Protein structures available at
284 doi.org/10.25451/flinders.21946034). Each of those models was individually docked
285 against all 3,223 predictions from the *B. cellulosilyticus* WH2 proteome available in the
286 AlphaFold database using hdock-lite. The PDB files for all the structural models and a
287 summary of the docking scores are provided in the supplemental material (Table S7).
288 The strongest predicted docking interactions were between *K. winsdale* protein RNA
289 polymerase subunit (gp47) with the bacterial transmembrane EamA-family transporter
290 (UniProt ID: A0A0P0GB77, hdock-score =-711), tail spike (gp22) with TonB-dependent
291 receptors (UniProtID: A0A0P0GGA2, hdock-score =-700), and transmembrane protein
292 (gp44) with outer membrane protein (UniProt ID: A0A0N7IEG6, hdock-score =-672).
293 Although 34 of the phage proteins bind to bacterial proteins named TonB receptors,
294 they each had unique UniProtID. The bacterial host, *B. cellulosilyticus* WH2 contains six
295 TonB homologs and 112 TonB-dependent transporters, similar to other *Bacteroides*
296 genomes. These transporters are typically used by *Bacteroides* to take up starches
297 (36), but we propose, based on structural modelling, that one or more of the TonB-
298 dependent receptors, are utilized by crAssphage to penetrate through the cell
299 membrane.

300 Figure 4: A) 3D structure of tail spike protein (gp22) from *K. winsdale* (Bc01) visualized
301 using PyMOL, B) 3D structure of tail spike protein (gp22) interaction (black) with TonB-
302 dependent receptor (yellow) from the bacterial host, *B. cellulosilyticus* WH2.

303 **Discussion**

304 The role of crAssphage in the human gut is enigmatic, partly because so few
305 crAssphages have been cultured (17). Here, we present three novel crAssphages
306 spanning three genera but infecting one *B. cellulosilyticus* WH2, which suggests that
307 these phages may not have co-evolved with their bacterial host, suggesting other
308 factors driving to crAssphage evolution. Functional characterization of these novel
309 species and comparison to other reference genomes revealed synteny across
310 crAssphage isolates, with a higher range of gene similarity observed within phage
311 belonging to the same taxa. Across the three novel species, we identified a single
312 structural gene encoding tail spike protein that was found in all three species and was
313 under purifying selection. Protein docking predicted that the tail spike protein binds to
314 the TonB-dependent transporter on the bacterial surface, which is a known receptor for
315 phage sensitivity, suggesting the tail spike protein plays a role in host specificity.

316 We isolated and classified the three novel crAssphages to family and genus level
317 classification (Figure 1), with two species in the *Steigviridae* family, that we named
318 *Kehishuvirus winsdale* (Bc01), and *Kolpuevirus frerule* (Bc03). *K. winsdale* (Bc01) is
319 closely related to the first crAssphage isolate, *K. primarius* (crAss001), while *K. frerule*
320 (Bc03) is the first pure culture isolate from its genus. Finally, the third species belongs to
321 a novel genus and species that we named *Rudgehvirus redwords* (Bc11). Whole

322 genomic comparison revealed synteny across all the crAssphage genomes with gene
323 order conserved, despite differences in gene similarity (Figure 2, Figure 3) as observed
324 Crassvirales order (16). As expected, isolates from the same family-level classification
325 have more gene similarity than across families (Figure 3). Within a family, conserved
326 genes include structural genes (MCP, terminase large subunit, portal, Integration Host
327 Factor (IHF), tail tubular and stabilization protein), replication machinery genes (DnaG
328 primase, DnaB helicases, SNF2 family, AAA+ superfamily and lysis genes), and
329 transcription genes (RNA polymerase subunits, nuclease of the PDDEXK family)
330 (Figure 3, Table S3, S4 and S5) (42) as observed in other crAssphages (16). The study
331 found that the crAssphage isolates within the *Steigviridae* family encoded DNA
332 polymerase A, while those within the *Intestiviridae* family encoded DNA polymerase B.
333 This observation is consistent with the DNA polymerase switching previously reported in
334 crAssphages(16). While some crAssphage isolates have been found to have
335 reassigned stop codons (30,33), none of the novel isolates in this study reassigned stop
336 codons by measuring coding density and the absence of suppressor tRNA (Table S2).
337 On the other hand, comparing the morphology of the three species showed differences
338 in capsid sizes relative to the reference crAssphage isolates. The capsid diameter was
339 larger in size, between 90 to 97 nm for the three species in this study (Figure 2)
340 compared to the reference genomes that were estimated to be 77 nm (22,24). We
341 confirmed this difference was not an artefact of how the capsid diameter was measured
342 by repeating the measurements for *K. primarius* (crAss001) and *J. secundus* (crAss002)
343 (Figure S4), and all the phages were negatively stained with uranyl acetate. In tailed
344 phages, the genome length is expected to increase as the cube of the capsid diameter,

345 because DNA is packaged at a constant density of about 0.5bp/nm² (37,38). However,
346 the two closely related genomes *K. primarius* (crAss001) and *K. winsdale* (Bc01) only
347 varied by 1,838 bp while *K. winsdale* capsid was 22% larger in diameter (94 nm versus
348 77 nm), displaying an internal volume that could accommodate 80,000 bp more than *K.*
349 *primarius* (crAss001). The difference in the capsid size could be attributed to the
350 variations in the scaffold protein, as observed in *Staphylococcus aureus* phages where
351 the same major capsid protein assembled within different scaffolding proteins generates
352 different capsid sizes (39,40). Two possible mechanisms might be responsible for filling
353 the additional internal volume of *K. winsdale* (Bc01). First, this species could follow a
354 headful packaging mechanism storing more DNA than just the viral genome length. This
355 packaging mechanism was predicted in *J. secundus* (crAss002) (24); nonetheless, the
356 absence of direct terminal repeats (Table 1) is uncommon in tailed phages using the
357 headful mechanism (41). Second, the presence of internal proteins in the capsid could
358 occupy the remaining volume, as shown in the capsid of *K. primarius* (crAss001)
359 genome (26).

360 Isolation of multiple crAssphages infecting the same host revealed that the tail spike
361 protein is conserved among crAssphages infecting the same host (Figure 3). Tail spike
362 proteins are important in tailed bacteriophages for binding to specific membrane
363 receptors on the bacteria (43). We also found evidence of purifying selection acting on
364 the tail spike protein, indicating its essential role in host specificity (Table 2). Using
365 structural modelling, we predicted that the tail spike protein interacts with the TonB-
366 dependent receptor on the bacterial surface, a gene that has been shown to play a
367 critical role in phage infection of Bacteroidota and other species (Porter et al., 2020;

368 Shkoporov, Khokhlova, et al., 2021). The interaction between crAssphage and TonB-
369 dependent receptors along with capsular polysaccharides has been shown to play a
370 role in the long-term persistence observed in these phages (25). TonB-dependent
371 receptors are involved in the uptake of various nutrients, including iron, which is an
372 essential element for many bacteria. By targeting these transporters, the crAssphage is
373 able to hijack the host's nutrient acquisition machinery such as capsular polysaccharide
374 biosynthesis for its own benefit, allowing it to persist and replicate within the host over a
375 longer period of time (25). Further, another study has shown that crAssphage RNA
376 polymerase and tail proteins were undergoing positive selection by comparing genomes
377 assembled from parent and infant fecal samples(44). However, in that study they didn't
378 characterize the crAssphage taxa or host, therefore the difference in the selection
379 pressure may be likely due to these external evolutionary pressures. We also suggest
380 that tail spike proteins can be used to cluster crAssphage genomes to groups that
381 potentially infect the same bacterial host.

382 Overall, in this study we identified and characterized three novel crAssphage species
383 isolates from wastewater and infecting the bacterial host *Bacteroides cellulosilyticus*
384 WH2. Our findings expand the known crAssphage isolates and provide insight into the
385 role of the tail proteins in host specificity and infection. Outcomes of these efforts
386 resulted in a unique model of three distinct crAssphages infecting the same strain which
387 can be now utilized experimentally to study one of the dominant members of the gut
388 microbiome, and how their interactions shape the gut microbiome.

389 **Methods**

390 **Phage sampling**

391 Untreated sewage water (influent) was collected from a waste treatment plant in Cardiff,
392 CA in 1L Nalgene bottles. Upon collection, the bottles were placed on ice and in the
393 dark for processing. An aliquot of 30 ml influent was put into a sterile 50 ml centrifuge
394 tube and centrifuged at 5,000 RCF for 5 min to pellet the debris. The supernatant was
395 decanted and passed through a 0.22 μ m Sterivex filter. The filtrate was used as a
396 phage source and stored between 2 to 8 $^{\circ}$ C.

397 **Host bacteria cultivation**

398 The bacterial strain, *B. cellulosilyticus* WH2 (45) was used as the bacterial host and was
399 received as glycerol stocks from Washington University, St. Louis. Bacteria were grown
400 in brain-heart infusion media supplemented with 2mM MgSO₄, and 10mM MgCl₂ we
401 denote as BHISMg. Culture plates were supplemented with 1.5% agar and incubated at
402 37 $^{\circ}$ C for 48 hours under anaerobic conditions with 5% H₂, 5% CO₂, and 90% N₂.
403 Following incubation, a sterile loop was used to transfer an isolated colony into a 12 hr
404 deoxygenated BHISMg broth. Following anaerobic incubation at 37 $^{\circ}$ C for 24 hours the
405 liquid cultures were further subcultured into another BHISMg broth and incubated
406 overnight.

407 **Plaque assays**

408 Plaque assays were performed with minor modifications described below. Before
409 beginning the plaque assays, BHISMg plates were deoxygenated for 12 hrs in the

410 anaerobic chamber and pre-warmed before use. For top agar plates, cooled molten
411 BHISMg with 0.7 % agar was inoculated with 500 μ l of bacteria, and between 2 μ l and
412 50 μ l of processed phage influent was overlayed onto BHISMg plates. The plates were
413 cooled for 15 minutes before incubating at 37°C for up to five days. Plates were
414 assessed daily for the development of plaques.

415 Lysate preparation

416 Plaque from each plate was inoculated into 200 μ l of SM buffer and homogenized to
417 diffuse the phage from the agar to the buffer. A 200 μ l aliquot of the phage was added
418 to *B. cellulosilyticus* WH2 bacteria in the log-growth phase and grown at 37°C
419 anaerobically, overnight. The tubes containing the bacteria and phage were manually
420 shaken every 30 min for the first three hours of incubation. Post incubation, tubes were
421 centrifuged at 4500 \times g for 5 min, and the supernatant was collected and concentrated
422 using a 50,000 kDa MWCO Vivaspin ultrafiltration unit (Sartorius). Phage lysate was
423 stored at 4°C.

424 Titering enumeration

425 Phage titering was undertaken using the molten agar overlay method described above.
426 A 200 μ l aliquot of the lysate was diluted 10-fold in sterile SM buffer, and 10 μ l was
427 spotted onto a BHISMg plate. The plates were incubated for 24-48 hr at 37 °C. After
428 incubation, the plates were analyzed by counting the plaques obtained and determining
429 the titer.

430 Viral DNA extraction and sequencing

431 DNA extractions were performed using the Phage DNA isolation kit (Norgen) as per
432 manufacturer instructions. In short, 1 ml of phage lysate was DNase I treated, lysed,
433 and treated with Proteinase K. The sample was added to a spin column and washed
434 three times. DNA was eluted in 75 μ l of the elution buffer. The second elution
435 recommended by the kit was not performed. The DNA obtained was quantified using a
436 Qubit 1x dsDNA high-sensitivity assay kit (Invitrogen, Life Technologies). For Oxford
437 Nanopore MinION sequencing the library preparation and sequencing were performed
438 using Oxford Nanopore Rapid Barcoding Sequencing Kit (SQK-RBK0004). The Illumina
439 sequencing libraries were prepared by extracting the total nucleic acid (RNA and DNA)
440 using the COBAS AmpliPrep instrument (Roche), with NEBNext library construction and
441 sequenced on Illumina MiSeq as described in (46). Eight of the samples were
442 sequenced on both Nanopore and Illumina sequencing platforms (Bc01 to Bc08), four
443 were sequenced only on Nanopore platforms (Bc09 to Bc12), and the remaining four
444 were sequenced only on Illumina platforms (Bc13 to Bc16). The sequencing data were
445 deposited to Sequence Read Archive in Bioproject, PRJNA737576.

446 For the Nanopore sequenced isolates, basecalling was performed with Guppy v6.0.1.
447 The reads were then processed with Filtlong v.0.2.20 (47) to remove reads less than
448 1,000 bp in length and exclude 5% of the lowest-quality reads. Similarly, Illumina
449 sequences were processed with prinseq++ (48), filtering reads less than 60 bp in length,
450 reads with quality scores less than 25, and exact duplicates.

451 Genome assembly

452 The steps for genome assembly are available as a pipeline based on Snakemake using
453 Snaketool (49) and available on GitHub (50).

454 Nanopore reads were assembled using Unicycler (51) and Flye (52), while Illumina
455 reads were assembled using MEGAHIT (53). These assemblers were selected as they
456 provide assembly graphs of the contigs assembled, which would be utilized for
457 completing fragmented genome assemblies, (54–58). To assess the quality of the
458 assembly, the resulting contigs were processed with ViralVerify to detect viral contigs
459 (59), read coverage was calculated using CoverM (60), and whether the contigs were
460 fragmented using assembly graph information. The assembly graph includes details of
461 connecting unitigs (high-quality contigs) that represent the longest non-branching paths
462 joined together to form contigs.

463 Unitigs that were greater than 90 kb, identified as viral, with the highest read coverage,
464 and described as complete (CheckV) were selected from each assembly. For each
465 genome, one representative unitig (higher quality contigs) was selected (circular,
466 longest contig with high read coverage) per sample, as the complete phage assembly.
467 In the end, the assemblies were polished with high-coverage Illumina reads using Polca
468 to reduce sequencing-related errors (61).

469 Taxonomic and functional annotation

470 The isolates in this study were processed with CrassUS (62). CrassUS was developed
471 specifically for annotating genomes from the Crassvirales order, incorporating a focused

472 database including known crAssphage genomes. This program generates a table of
473 taxa annotations, functional annotations, the presence of direct terminal repeats (DTR),
474 and average nucleotide identities of the most similar reference genomes. Taxonomic
475 annotations from CrassUS were used, as they follow the ICTV (27,29) Crassvirales
476 order demarcation criteria to determine taxonomy. The three conserved genes across
477 crAssphages including major capsid protein (MCP), portal protein, and terminase large
478 subunit (*terL*) were used to build the phylogenetic trees. The phylogenetic trees were
479 plotted in iTol (63). The predicted genes and their arrangement across species were
480 visualized using clinker plots (64), after re-circularizing the genes to start at the *terL* in
481 order to examine synteny across the phage genomes assembled. Finally, phages may
482 encode their own tRNA genes escaping the host translation machinery, and these were
483 predicted with tRNA-scanSE (65).

484 Transmission electron microscopy imaging

485 Bacteroides phages were grown using the phage overlay method described above.
486 Phage lysates were diluted 1:10, and 5 μ L of the diluted phage lysate was applied to a
487 plasma-cleaned grid for two minutes at room temperature. The grids were formvar and
488 carbon coated 200 mesh grids and they were plasma cleaned using the Gatan (Solarus)
489 Advanced plasma system for 30 sec prior to use. The excess phage lysate sample was
490 wicked off with Whatman filter paper and the grid was washed with 5 μ L of water. The
491 sample was negatively stained with 5 μ L of the 2 % w/v uranyl acetate for 1 minute. The
492 excess stain was wicked off with filter paper to dry the sample on the grid. The grid was
493 then imaged using a Tecnai G2 Spirit TEM operated at 120kV at a magnification of

494 49,000x and the images were recorded on an AMT Nanosprint 15 digital camera using
495 software v7.0.1.

496 Phage measurements were calculated using the ImageJ software (66). The capsid
497 diameter was measured by obtaining the diameter of the circle circumscribing the
498 capsid, such that the more distant vertices of the projected capsid contacted the circle
499 (Figure S3). For the tail, the length was calculated from the base of the capsid to the
500 end of the visible tail, including the collar section of the phage structure. Tail fibres or
501 appendages were not calculated (Figure S3). Average measurements from 5 phages
502 were calculated and reported. The TEM image was further edited for publication using
503 the GNU Image Manipulation Program (GIMP) (67).

504 Evolutionary analyses

505 The 14 crAssphage isolated and sequenced in this study and the four reference pure
506 culture isolates, *K. primarius* (crAss001), *W. bangladeshii* (DAC15), *Wulffhauvirus*
507 *isolate* (DAC17), and *J. secundus* (crAss002) were assessed together for this analysis.
508 Orthologous genes were identified from genes predicted from the above 18 genomes,
509 using Orthofinder (68). Orthogroups that included genes that were only present in
510 phages from the host—*B. cellulosilyticus* WH2—were assessed further for signatures of
511 host specificity.

512 These orthogroups were aligned using Muscle (69) codon-based multiple sequence
513 alignment in MEGA11 (70). To test for codon-based positive selection, we calculated
514 the probability of rejecting the null hypothesis of strict neutrality ($d_N = d_S$), and in favour
515 of the alternate hypothesis ($d_N > d_S$). The d_N/d_S values were calculated from the MSA

516 using MEGA v.11.0 (71), with the Li-Wu-Luo method (72). The variance of the
517 difference was computed using bootstraps, set to 100 replicates.

518 Predicting proteins 3D structure and docking

519 The 3D structures of the proteins from *K. winsdale* (Bc01), *K. frurule* (Bc03), and *R.*
520 *redwords* (Bc11) were predicted using Colabfold version 1.4.0 (35) on the Gadi server
521 at the National Computational Infrastructure (NCI). The previously predicted 3D protein
522 structures of all the proteins for *B. cellulosilyticus* WH2 were downloaded from the
523 AlphaFold Protein Structure Database via the Google Cloud Platform (73). All protein
524 pairs were docked using hdock-lite version 1.1 (74) on the Gadi server. The results from
525 hdock were sorted based on the binding score in the output file to identify the highest-
526 quality binding predictions for each phage protein. The 3D structure of the proteins were
527 visualized using PyMOL.

528 Data availability

529 The samples were submitted to Sequence Read Archive within the project,
530 PRJNA737576. *B. cellulosilyticus* WH2, *K. winsdale* (Bc01), *K. frurule* (Bc03), and *R.*
531 *redwords* (Bc11) are all available on Genbank with accessions QQ198717 (Bc01),
532 QQ198718 (Bc03), and QQ198719 (Bc11), and we are working on making them
533 available through ATCC. The 3D protein structures for the three crAssphage genomes
534 are available to download at doi.org/10.25451/flinders.21946034.

535 Author Contributions

536 BNP performed bioinformatics analysis, wrote the paper, analyzed the genomes. AV,
537 CS, CC, WP, NJ SG collected samples, isolated and cultured phages. MFM, CS, MA,
538 KP, LD sequenced phages. CL, SG took TEM images. KM, MR, PD, SRG, VM, GB, AL,
539 SH performed bioinformatics analysis. AMS, EAD, RAE conceived the project,
540 performed the bioinformatics, and wrote the paper with input from all authors.

541 **Acknowledgments**

542 This research/project was undertaken with the assistance of resources and services
543 from Flinders University and the National Computational Infrastructure (NCI), which is
544 supported by the Australian Government.

545 **Funding**

546 This work was supported by an award from NIH NIDDK RC2DK116713 and an award
547 from the Australian Research Council DP220102915. PD's contribution was supported
548 by the Polish National Agency for Academic Exchange (NAWA) Bekker Program
549 fellowship no. BPN/BEK/2021/1/00416.

550 **References**

- 551 1. Hou K, Wu Z-X, Chen X-Y, Wang J-Q, Zhang D, Xiao C, et al. Microbiota in health
552 and diseases. *Signal Transduct Target Ther* [Internet]. 2022 Apr 23;7(1):135.
553 Available from: <http://dx.doi.org/10.1038/s41392-022-00974-4>
- 554 2. Integrative HMP (iHMP) Research Network Consortium. The Integrative Human
555 Microbiome Project. *Nature* [Internet]. 2019 May;569(7758):641–8. Available from:
556 <http://dx.doi.org/10.1038/s41586-019-1238-8>
- 557 3. Shamash M, Maurice CF. Phages in the infant gut: a framework for virome
558 development during early life. *ISME J* [Internet]. 2022 Feb;16(2):323–30. Available

559 from: <http://dx.doi.org/10.1038/s41396-021-01090-x>

560 4. Hugenholtz P, Goebel BM, Pace NR. Impact of culture-independent studies on the
561 emerging phylogenetic view of bacterial diversity. *J Bacteriol* [Internet]. 1998
562 Sep;180(18):4765–74. Available from: <http://dx.doi.org/10.1128/JB.180.18.4765-4774.1998>

563

564 5. Pace NR, Stahl DA, Lane DJ, Olsen GJ. The Analysis of Natural Microbial
565 Populations by Ribosomal RNA Sequences. In: Marshall KC, editor. *Advances in*
566 *Microbial Ecology* [Internet]. Boston, MA: Springer US; 1986. p. 1–55. Available
567 from: https://doi.org/10.1007/978-1-4757-0611-6_1

568 6. Inglis LK, Edwards RA. How Metagenomics Has Transformed Our Understanding
569 of Bacteriophages in Microbiome Research. *Microorganisms* [Internet]. 2022 Aug
570 19;10(8). Available from: <http://dx.doi.org/10.3390/microorganisms10081671>

571 7. Roach M, Beecroft S, Mihindukulasuriya KA, Wang L, Lima LFO, Dinsdale EA, et
572 al. Hecatomb: An End-to-End Research Platform for Viral Metagenomics [Internet].
573 *bioRxiv*. 2022 [cited 2022 Nov 22]. p. 2022.05.15.492003. Available from:
574 <https://www.biorxiv.org/content/biorxiv/early/2022/05/16/2022.05.15.492003>

575 8. Hesse RD, Roach M, Kerr EN, Papudeshi B, Lima LFO, Goodman AZ, et al. Phage
576 Diving: An Exploration of the Carcharhinid Shark Epidermal Virome. *Viruses*
577 [Internet]. 2022 Sep 5;14(9). Available from: <http://dx.doi.org/10.3390/v14091969>

578 9. Anthenelli M, Jasien E, Edwards R, Bailey B, Felts B, Katira P, et al. Phage and
579 bacteria diversification through a prophage acquisition ratchet [Internet]. *bioRxiv*.
580 2020 [cited 2022 Jul 19]. p. 2020.04.08.028340. Available from:
581 <https://www.biorxiv.org/content/10.1101/2020.04.08.028340v1>

582 10. Knowles B, Silveira CB, Bailey BA, Barott K, Cantu VA, Cobián-Güemes AG, et al.
583 Lytic to temperate switching of viral communities. *Nature* [Internet]. 2016 Mar
584 24;531(7595):466–70. Available from: <http://dx.doi.org/10.1038/nature17193>

585 11. Chevallereau A, Pons BJ, van Houte S, Westra ER. Interactions between bacterial
586 and phage communities in natural environments. *Nat Rev Microbiol* [Internet]. 2022
587 Jan;20(1):49–62. Available from: <http://dx.doi.org/10.1038/s41579-021-00602-y>

588 12. Silveira CB, Luque A, Rohwer F. The landscape of lysogeny across microbial
589 community density, diversity and energetics. *Environ Microbiol* [Internet]. 2021
590 Aug;23(8):4098–111. Available from: <http://dx.doi.org/10.1111/1462-2920.15640>

591 13. Qin J, Li R, Raes J, Arumugam M, Burgdorf KS, Manichanh C, et al. A human gut
592 microbial gene catalogue established by metagenomic sequencing. *Nature*
593 [Internet]. 2010 Mar 4;464(7285):59–65. Available from:
594 <http://dx.doi.org/10.1038/nature08821>

595 14. HMP Consortium. Structure, function and diversity of the healthy human

596 microbiome. *Nature* [Internet]. 2012 Jun 13 [cited 2022 Jul 25];486(7402):207–14.
597 Available from: <https://www.nature.com/articles/nature11234>

598 15. Pargin E, Roach M, Skye A, Edwards R, Giles S. The human gut virome:
599 Composition, colonisation, interactions, and impacts on human health [Internet].
600 2022. Available from: <http://dx.doi.org/10.31219/osf.io/s9px2>

601 16. Yutin N, Benler S, Shmakov SA, Wolf YI, Tolstoy I, Rayko M, et al. Analysis of
602 metagenome-assembled viral genomes from the human gut reveals diverse
603 putative CrAss-like phages with unique genomic features. *Nat Commun* [Internet].
604 2021 Feb 16;12(1):1044. Available from: <http://dx.doi.org/10.1038/s41467-021-21350-w>

606 17. Edwards RA, Vega AA, Norman HM, Ohaeri M, Levi K, Dinsdale EA, et al. Global
607 phylogeography and ancient evolution of the widespread human gut virus
608 crAssphage. *Nat Microbiol* [Internet]. 2019 Oct;4(10):1727–36. Available from:
609 <http://dx.doi.org/10.1038/s41564-019-0494-6>

610 18. Rossi A, Treu L, Toppo S, Zschach H, Campanaro S, Dutilh BE. Evolutionary Study
611 of the Crassphage Virus at Gene Level. *Viruses* [Internet]. 2020 Sep 17;12(9).
612 Available from: <http://dx.doi.org/10.3390/v12091035>

613 19. Norman JM, Handley SA, Baldridge MT, Droit L, Liu CY, Keller BC, et al. Disease-
614 specific alterations in the enteric virome in inflammatory bowel disease. *Cell*
615 [Internet]. 2015 Jan 29;160(3):447–60. Available from:
616 <http://dx.doi.org/10.1016/j.cell.2015.01.002>

617 20. Dutilh BE, Cassman N, McNair K, Sanchez SE, Silva GGZ, Boling L, et al. A highly
618 abundant bacteriophage discovered in the unknown sequences of human faecal
619 metagenomes. *Nat Commun* [Internet]. 2014 Jul 24;5:4498. Available from:
620 <http://dx.doi.org/10.1038/ncomms5498>

621 21. Guerin E, Shkoporov A, Stockdale SR, Clooney AG, Ryan FJ, Sutton TDS, et al. Biology
622 and Taxonomy of crAss-like Bacteriophages, the Most Abundant Virus in
623 the Human Gut. *Cell Host Microbe* [Internet]. 2018 Nov 14;24(5):653-664.e6.
624 Available from: <http://dx.doi.org/10.1016/j.chom.2018.10.002>

625 22. Shkoporov AN, Khokhlova EV, Fitzgerald CB, Stockdale SR, Draper LA, Ross RP,
626 et al. Φ CrAss001 represents the most abundant bacteriophage family in the human
627 gut and infects *Bacteroides intestinalis*. *Nat Commun* [Internet]. 2018 Nov
628 14;9(1):4781. Available from: <http://dx.doi.org/10.1038/s41467-018-07225-7>

629 23. Hryckowian AJ, Merrill BD, Porter NT, Van Treuren W, Nelson EJ, Garlena RA, et
630 al. *Bacteroides thetaiotaomicron*-Infecting Bacteriophage Isolates Inform
631 Sequence-Based Host Range Predictions. *Cell Host Microbe* [Internet]. 2020 Sep
632 9;28(3):371-379.e5. Available from: <http://dx.doi.org/10.1016/j.chom.2020.06.011>

633 24. Guerin E, Shkoporov AN, Stockdale SR, Comas JC, Khokhlova EV, Clooney AG, et

634 al. Isolation and characterisation of ΦcrAss002, a crAss-like phage from the human
635 gut that infects *Bacteroides xyloisolvans*. *Microbiome* [Internet]. 2021 Apr
636 12;9(1):89. Available from: <http://dx.doi.org/10.1186/s40168-021-01036-7>

637 25. Shkoporov AN, Khokhlova EV, Stephens N, Hueston C, Seymour S, Hryckowian
638 AJ, et al. Long-term persistence of crAss-like phage crAss001 is associated with
639 phase variation in *Bacteroides intestinalis*. *BMC Biol* [Internet]. 2021 Aug
640 18;19(1):163. Available from: <http://dx.doi.org/10.1186/s12915-021-01084-3>

641 26. Antson A, Bayfield O, Shkoporov A, Yutin N, Khokhlova E, Smith J, et al. Structural
642 atlas of the most abundant human gut virus [Internet]. Research Square. 2022.
643 Available from: <https://www.researchsquare.com/article/rs-1898492/v1>

644 27. Shkoporov AN, Stockdale SR, Adriaenssens EM, Yutin N, Koonin EV, Dutilh BE, et
645 al. Create one new order (Crassvirales) including four new families, ten new
646 subfamilies, 42 new genera and 73 new species (Caudoviricetes) [Internet]. 2021.
647 Available from: <https://ictv.global/ictv/proposals/2021.022B.R.Crassvirales.zip>

648 28. Dutilh BE, Varsani A, Tong Y, Simmonds P, Sabanadzovic S, Rubino L, et al.
649 Perspective on taxonomic classification of uncultivated viruses. *Curr Opin Virol*
650 [Internet]. 2021 Dec;51:207–15. Available from:
651 <http://dx.doi.org/10.1016/j.coviro.2021.10.011>

652 29. Walker PJ, Siddell SG, Lefkowitz EJ, Mushegian AR, Adriaenssens EM, Alfenas-
653 Zerbini P, et al. Recent changes to virus taxonomy ratified by the International
654 Committee on Taxonomy of Viruses (2022). *Arch Virol* [Internet]. 2022
655 Nov;167(11):2429–40. Available from: <http://dx.doi.org/10.1007/s00705-022-05516-5>

657 30. Borges AL, Lou YC, Sachdeva R, Al-Shayeb B, Jaffe AL, Lei S, et al. Stop codon
658 recoding is widespread in diverse phage lineages and has the potential to regulate
659 translation of late stage and lytic genes [Internet]. *bioRxiv*. 2021 [cited 2022 Jul 23].
660 p. 2021.08.26.457843. Available from:
661 <https://www.biorxiv.org/content/biorxiv/early/2021/08/26/2021.08.26.457843>

662 31. Ivanova NN, Schwientek P, Tripp HJ, Rinke C, Pati A, Huntemann M, et al. Stop
663 codon reassessments in the wild. *Science* [Internet]. 2014 May 23;344(6186):909–
664 13. Available from: <http://dx.doi.org/10.1126/science.1250691>

665 32. Crisci MA, Chen L-X, Devoto AE, Borges AL, Bordin N, Sachdeva R, et al. Closely
666 related Lak megaphages replicate in the microbiomes of diverse animals. *iScience*
667 [Internet]. 2021 Aug 20;24(8):102875. Available from:
668 <http://dx.doi.org/10.1016/j.isci.2021.102875>

669 33. Peters SL, Borges AL, Giannone RJ, Morowitz MJ, Banfield JF, Hettich RL.
670 Experimental validation that human microbiome phages use alternative genetic
671 coding. *Nat Commun* [Internet]. 2022 Sep 29;13(1):5710. Available from:
672 <http://dx.doi.org/10.1038/s41467-022-32979-6>

673 34. Altschul SF, Gish W, Miller W, Myers EW, Lipman DJ. Basic local alignment search
674 tool. *J Mol Biol* [Internet]. 1990 Oct 5;215(3):403–10. Available from:
675 [http://dx.doi.org/10.1016/S0022-2836\(05\)80360-2](http://dx.doi.org/10.1016/S0022-2836(05)80360-2)

676 35. Mirdita M, Schütze K, Moriwaki Y, Heo L, Ovchinnikov S, Steinegger M. ColabFold:
677 making protein folding accessible to all. *Nat Methods* [Internet]. 2022
678 Jun;19(6):679–82. Available from: <http://dx.doi.org/10.1038/s41592-022-01488-1>

679 36. Pollet RM, Martin LM, Koropatkin NM. TonB-dependent transporters in the
680 Bacteroidetes: Unique domain structures and potential functions. *Mol Microbiol*
681 [Internet]. 2021 Mar;115(3):490–501. Available from:
682 <http://dx.doi.org/10.1111/mmi.14683>

683 37. Luque A, Benler S, Lee DY, Brown C, White S. The Missing Tailed Phages:
684 Prediction of Small Capsid Candidates. *Microorganisms* [Internet]. 2020 Dec
685 8;8(12). Available from: <http://dx.doi.org/10.3390/microorganisms8121944>

686 38. Lee DY, Bartels C, McNair K, Edwards RA, Swairjo MA, Luque A. Predicting the
687 capsid architecture of phages from metagenomic data. *Comput Struct Biotechnol J*
688 [Internet]. 2022 Jan 5;20:721–32. Available from:
689 <http://dx.doi.org/10.1016/j.csbj.2021.12.032>

690 39. Spilman MS, Damle PK, Dearborn AD, Rodenburg CM, Chang JR, Wall EA, et al.
691 Assembly of bacteriophage 80 α capsids in a *Staphylococcus aureus* expression
692 system. *Virology* [Internet]. 2012 Dec 20;434(2):242–50. Available from:
693 <http://dx.doi.org/10.1016/j.virol.2012.08.031>

694 40. Dearborn AD, Wall EA, Kizziah JL, Klenow L, Parker LK, Manning KA, et al.
695 Competing scaffolding proteins determine capsid size during mobilization of
696 *Staphylococcus aureus* pathogenicity islands. *eLife* [Internet]. 2017 Oct 6;6.
697 Available from: <http://dx.doi.org/10.7554/eLife.30822>

698 41. Casjens SR, Gilcrease EB. Determining DNA packaging strategy by analysis of the
699 termini of the chromosomes in tailed-bacteriophage virions. *Methods Mol Biol*
700 [Internet]. 2009;502:91–111. Available from: http://dx.doi.org/10.1007/978-1-60327-565-1_7

702 42. Weinheimer AR, Aylward FO. A distinct lineage of Caudovirales that encodes a
703 deeply branching multi-subunit RNA polymerase. *Nat Commun* [Internet]. 2020 Sep
704 9;11(1):4506. Available from: <http://dx.doi.org/10.1038/s41467-020-18281-3>

705 43. Nobrega FL, Vlot M, de Jonge PA, Dreesens LL, Beaumont HJE, Lavigne R, et al.
706 Targeting mechanisms of tailed bacteriophages. *Nat Rev Microbiol* [Internet]. 2018
707 Dec;16(12):760–73. Available from: <http://dx.doi.org/10.1038/s41579-018-0070-8>

708 44. Brown BP, Chopera D, Havyarimana E, Wendoh J, Jaumdally S, Nyangahu DD, et
709 al. crAssphage genomes identified in fecal samples of an adult and infants with
710 evidence of positive genomic selective pressure within tail protein genes. *Virus Res*

711 [Internet]. 2021 Jan 15;292:198219. Available from:
712 <http://dx.doi.org/10.1016/j.virusres.2020.198219>

713 45. McNulty NP, Wu M, Erickson AR, Pan C, Erickson BK, Martens EC, et al. Effects of
714 diet on resource utilization by a model human gut microbiota containing
715 *Bacteroides cellulosilyticus* WH2, a symbiont with an extensive glycobiome. *PLoS*
716 *Biol* [Internet]. 2013 Aug 20;11(8):e1001637. Available from:
717 <http://dx.doi.org/10.1371/journal.pbio.1001637>

718 46. Kim AH, Armah G, Dennis F, Wang L, Rodgers R, Droit L, et al. Enteric virome
719 negatively affects seroconversion following oral rotavirus vaccination in a
720 longitudinally sampled cohort of Ghanaian infants. *Cell Host Microbe* [Internet].
721 2022 Jan 12;30(1):110-123.e5. Available from:
722 <http://dx.doi.org/10.1016/j.chom.2021.12.002>

723 47. Wick RR. Filtlong: Tool for filtering long reads by quality [Internet]. 2018. Available
724 from: <https://github.com/rrwick/Filtlong/>

725 48. Cantu VA, Sadural J, Edwards R. PRINSEQ++, a multi-threaded tool for fast and
726 efficient quality control and preprocessing of sequencing datasets [Internet]. *PeerJ*
727 *Preprints*; 2019 Feb [cited 2022 Jul 24]. Report No.: e27553v1. Available from:
728 <https://peerj.com/preprints/27553v1/>

729 49. Roach M, Pierce-Ward NT, Schecki R, Mallawaarachchi V, Papudeshi B, Handley
730 SA, et al. Ten simple rules and a template for creating workflows-as-applications
731 [Internet]. 2022. Available from: <http://dx.doi.org/10.31219/osf.io/8w5j3>

732 50. Papudeshi B, Mallawaarachchi V, Roach M, Edwards R. spaE: Phage genome
733 assembly and annotation [Internet]. 2022. Available from:
734 <https://github.com/linsalrob/spae>

735 51. Wick RR, Judd LM, Gorrie CL, Holt KE. Unicycler: Resolving bacterial genome
736 assemblies from short and long sequencing reads. *PLoS Comput Biol* [Internet].
737 2017 Jun;13(6):e1005595. Available from:
738 <http://dx.doi.org/10.1371/journal.pcbi.1005595>

739 52. Kolmogorov M, Yuan J, Lin Y, Pevzner PA. Assembly of long, error-prone reads
740 using repeat graphs. *Nat Biotechnol* [Internet]. 2019 May;37(5):540–6. Available
741 from: <http://dx.doi.org/10.1038/s41587-019-0072-8>

742 53. Li D, Luo R, Liu C-M, Leung C-M, Ting H-F, Sadakane K, et al. MEGAHIT v1.0: A
743 fast and scalable metagenome assembler driven by advanced methodologies and
744 community practices. *Methods* [Internet]. 2016 Jun 1;102:3–11. Available from:
745 <http://dx.doi.org/10.1016/j.ymeth.2016.02.020>

746 54. Wick RR, Schultz MB, Zobel J, Holt KE. Bandage: interactive visualization of de
747 novo genome assemblies. *Bioinformatics* [Internet]. 2015 Oct 15;31(20):3350–2.
748 Available from: <http://dx.doi.org/10.1093/bioinformatics/btv383>

749 55. Bruce T, De Wardt R, Papudeshi B, Robinson B, Cuevas DA, Aguinaldo K, et al.
750 The intersection of genotype and phenotype: Informing ecotype development.

751 56. Mallawaarachchi V, Wickramarachchi A, Lin Y. GraphBin: refined binning of
752 metagenomic contigs using assembly graphs. *Bioinformatics* [Internet]. 2020 Jun
753 1;36(11):3307–13. Available from: <http://dx.doi.org/10.1093/bioinformatics/btaa180>

754 57. Mallawaarachchi VG, Lin Y. Metacoag: Binning metagenomic contigs via
755 composition, coverage and assembly graphs. *Res Comput Mol Biol* [Internet].
756 2022; Available from: https://link.springer.com/chapter/10.1007/978-3-031-04749-7_5

758 58. Mallawaarachchi VG, Wickramarachchi AS, Lin Y. GraphBin2: refined and
759 overlapped binning of metagenomic contigs using assembly graphs. *WASA*
760 [Internet]. 2020; Available from:
761 <https://drops.dagstuhl.de/opus/volltexte/2020/12797/>

762 59. Raiko M. viralVerify: viral contig verification tool [Internet]. 2021. Available from:
763 <https://github.com/ablab/viralVerify>

764 60. Woodcroft BJ. CoverM:DNA read coverage and relative abundance calculator
765 [Internet]. 2021. Available from: <https://github.com/wwood/CoverM>

766 61. Zimin AV, Salzberg SL. The genome polishing tool POLCA makes fast and
767 accurate corrections in genome assemblies. *PLoS Comput Biol* [Internet]. 2020
768 Jun;16(6):e1007981. Available from: <http://dx.doi.org/10.1371/journal.pcbi.1007981>

769 62. Carrillo D. CrassUS - Crassvirales Uncovering Software [Internet]. 2022. Available
770 from: <https://github.com/dcarrillox/CrassUS>

771 63. Letunic I, Bork P. Interactive Tree Of Life (iTOL) v4: recent updates and new
772 developments. *Nucleic Acids Res* [Internet]. 2019 Jul 2;47(W1):W256–9. Available
773 from: <http://dx.doi.org/10.1093/nar/gkz239>

774 64. Gilchrist CLM, Chooi Y-H. Clinker & clustermap.js: Automatic generation of gene
775 cluster comparison figures. *Bioinformatics* [Internet]. 2021 Jan 18; Available from:
776 <http://dx.doi.org/10.1093/bioinformatics/btab007>

777 65. Chan PP, Lowe TM. tRNAscan-SE: Searching for tRNA Genes in Genomic
778 Sequences. *Methods Mol Biol* [Internet]. 2019;1962:1–14. Available from:
779 http://dx.doi.org/10.1007/978-1-4939-9173-0_1

780 66. Schneider CA, Rasband WS, Eliceiri KW. NIH Image to ImageJ: 25 years of image
781 analysis. *Nat Methods* [Internet]. 2012 Jul;9(7):671–5. Available from:
782 <http://dx.doi.org/10.1038/nmeth.2089>

783 67. The GIMP Development Team. GIMP [Internet]. 2019. Available from:
784 <https://www.gimp.org>

785 68. Emms DM, Kelly S. OrthoFinder: phylogenetic orthology inference for comparative
786 genomics. *Genome Biol* [Internet]. 2019 Nov 14;20(1):238. Available from:
787 <http://dx.doi.org/10.1186/s13059-019-1832-y>

788 69. Edgar RC. High-accuracy alignment ensembles enable unbiased assessments of
789 sequence homology and phylogeny [Internet]. bioRxiv. 2022 [cited 2022 Aug 30]. p.
790 2021.06.20.449169. Available from:
791 <https://www.biorxiv.org/content/10.1101/2021.06.20.449169v2>

792 70. Stecher G, Tamura K, Kumar S. Molecular Evolutionary Genetics Analysis (MEGA)
793 for macOS. *Mol Biol Evol* [Internet]. 2020 Apr 1;37(4):1237–9. Available from:
794 <http://dx.doi.org/10.1093/molbev/msz312>

795 71. Tamura K, Stecher G, Kumar S. MEGA11: Molecular Evolutionary Genetics
796 Analysis Version 11. *Mol Biol Evol* [Internet]. 2021 Jun 25;38(7):3022–7. Available
797 from: <http://dx.doi.org/10.1093/molbev/msab120>

798 72. Li WH, Wu CI, Luo CC. A new method for estimating synonymous and
799 nonsynonymous rates of nucleotide substitution considering the relative likelihood
800 of nucleotide and codon changes. *Mol Biol Evol* [Internet]. 1985 Mar;2(2):150–74.
801 Available from: <http://dx.doi.org/10.1093/oxfordjournals.molbev.a040343>

802 73. Varadi M, Anyango S, Deshpande M, Nair S, Natassia C, Yordanova G, et al.
803 AlphaFold Protein Structure Database: massively expanding the structural
804 coverage of protein-sequence space with high-accuracy models. *Nucleic Acids Res*
805 [Internet]. 2022 Jan 7;50(D1):D439–44. Available from:
806 <http://dx.doi.org/10.1093/nar/gkab1061>

807 74. Yan Y, Tao H, He J, Huang S-Y. The HDOCK server for integrated protein-protein
808 docking. *Nat Protoc* [Internet]. 2020 May;15(5):1829–52. Available from:
809 <http://dx.doi.org/10.1038/s41596-020-0312-x>

810

811 **Supplementary Figures**

812 Figure S1: Genome coverage of the sequenced reads across samples. A) Genome
813 coverage in Nanopore sequenced reads, B) Genome coverage in Illumina sequenced
814 reads. The samples with * in red were not sequenced on the platform, and * in black
815 didn't produce a complete phage contig

816

817 Figure S2: Showing the taxa classification of the three novel species remains consistent
818 across the three conserved proteins A) Major capsid protein (MCP), B) portal protein C)
819 terminase large subunit (*terL*). The outgroup across all three trees set to *Cellulophaga*
820 *phage phi13:2*. The placement of the three novel species are highlighted on the tree,
821 Bc01 belonging to *Kehishuvirus* genera (light blue), Bc03 belonging to *Kolpuevirus*
822 genera (purple), and Bc11 belonging to a novel genus named *Rudgehvirus* (brown).

823

824 Figure S3: TEM phage measurements were taken for A) Capsid diameter, by drawing a
825 circle around the polygon with the edges within the circle. The diameter of this circle
826 was measured and represented as the capsid diameter. B) For tail length, a line was
827 drawn from the base of the capsid to the visible edge of the tail fibers. This was
828 repeated over five phages of the same sample and an average with standard deviation
829 was calculated across all of them

830

831 Figure S4: TEM measurements of capsids of A) *K. primarius* (crAss001) image from
832 (Shkorporov et al. 2018) measured to be 81 ± 2 nm and B) *J. secundus* (crAss002)
833 images from (Guerin et al. 2021) measured to be 75 ± 3 nm using ImageJ software. The
834 scale bar on both figures represents 100nm.

835 **Supplementary Tables**

836 Table S1: Phage genome assembly overview

837

838 Table S2: Coding density and search for tRNA suppressors within the three Bc
839 genomes

840

841 Table S3: *Kehishuvirus winsdale* (Bc01) functional annotation from crassus
842

843 Table S4: *Kolpuevirus frerule* (Bc03) functional annotation from crassus

844

845 Table S5: *Rudgehvirus redwords* (Bc11) functional annotation from crassus

846

847 Table S6: Orthologous groups identified across the 18 crAssphage isolates, highlighted
848 the two orthogroups that are present within the 14 crAssphage isolates from this study,
849 infecting the same bacterial host.

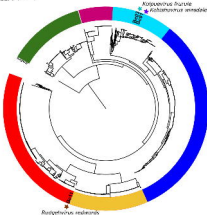
850

851 Table S7: Summary of the *Kehishuvirus winsdale* (Bc01) proteins interacting with
852 *Bacteroides cellulosilyticus* WH2 proteins using hdock-lite.

Genome	length (bp)	GC %	Coding density	Number of CDS	Unknown function	tRNA	DTR	Taxa
<i>Bc01</i>	100,841	35.09	91.84	104	58	24	False	<i>Kehishuvirus winsdale</i>
<i>Bc03</i>	99,523	33.00	92.06	108	63	5	False	<i>Kolpuevirus ffurule</i>
<i>Bc11</i>	90,575	29.15	87.45	84	48	0	False	<i>Rudgehvirus redwords</i>

ORTHOGROUP	Gene Function	Number Of Sequences	D _n /D _s	P Value	Z Statistic
OG0000000	Structural protein (gp23)	20	0.96	0.29	0.56
OG0000008*	Tail spike protein (gp22)	14	0.26	<0.001	9.15

Tree scale: 1.000000

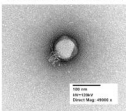


Portal gene - Family level

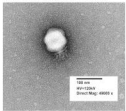
- Integviridae
- Covarrividae
- Sphaeriviridae
- Sipoviridae
- Epsilon
- Zeta

A1

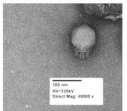
Kenilworth virus winsdale (Bc01)



Koipuevirus furule (Bc03)

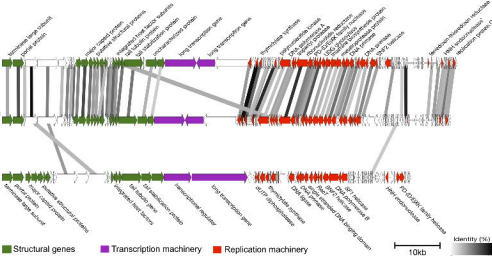


Ridgeovirus redwords (Bc11)



B)

Kehishuvirus windscale (Bo01)



Kolpovirus frunule (Be03)

Ridgehavirus redwords (Bc11)

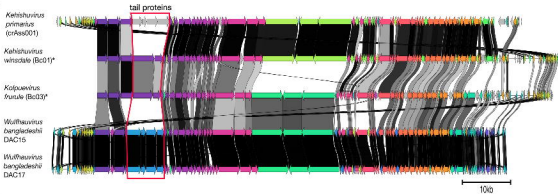
■ Structural genes

■ Transcription machinery

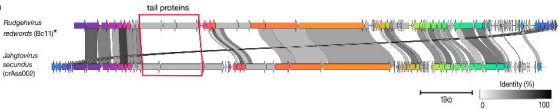
■ Replication machinery

Identity (%)

A)



B)



A)



B)

